Article

Systematic Comparison of ORC and s-CO$_2$ Combined Heat and Power Plants for Energy Harvesting in Industrial Gas Turbines

Maria Alessandra Ancona *, Michele Bianchi, Lisa Branchini, Andrea De Pascale, Francesco Melino, Antonio Peretto and Noemi Torricelli

Department of Industrial Engineering—DIN, University of Bologna, Viale del Risorgimento 2, 240136 Bologna, Italy; michele.bianchi@unibo.it (M.B.); lisa.branchini2@unibo.it (L.B.); andrea.depascale@unibo.it (A.D.P.); francesco.melino@unibo.it (F.M.); antonio.peretto@unibo.it (A.P.); noemi.torricelli2@unibo.it (N.T.)
* Correspondence: maria.ancona2@unibo.it

Abstract: Gas turbine power plants are widely employed with constrained efficiency in the industrial field, where they often work under variable load conditions caused by variations in demand, leading to fluctuating exhaust gas temperatures. Suitable energy harvesting solutions can be identified in bottoming cycles, such as the conventional Organic Rankine Cycles (ORC) or the innovative supercritical CO$_2$ (s-CO$_2$) systems. This paper presents a detailed comparison of the potential of ORC and s-CO$_2$ as bottomers of industrial gas turbines in a Combined Heat and Power (CHP) configuration. Different gas turbine models, covering the typical industrial size range, are taken into account and both full- and part-load operations are considered. Performance, component dimensions, and operating costs are investigated, considering ORC and s-CO$_2$ systems specifics in line with the current state-of-the-art products, experience, and technological limits. Results of the study show that the s-CO$_2$ could be more appropriate for CHP applications. Both the electric and thermal efficiency of s-CO$_2$ bottoming cycle show higher values compared with ORC, also due to the fact that in the examined s-CO$_2$ solution, the cycle pressure ratio is not affected by the thermal user temperature. At part-load operation, the gas turbine regulation strategy affects the energy harvesting performance in a CHP arrangement. The estimated total plant investment cost results to be higher for the s-CO$_2$, caused by the higher size of the heat recovery heat exchanger but also by the high specific investment cost still associated to this component. This point seems to make the s-CO$_2$ not profitable as the ORC solution for industrial gas turbine heat recovery applications. Nevertheless, a crucial parameter determining the feasibility of the investment is the prospective carbon tax application.

Keywords: supercritical CO$_2$; ORC; gas turbines; heat recovery; part-load; CHP; design; economic analysis

1. Introduction

The availability of natural gas at relatively low cost and the intensification of environmental regulations on air pollutants and CO$_2$ emissions have resulted in a shift toward gas-based power generation [1] which, in turn, is leading to the growth in Gas Turbine (GT) market. Nowadays, GTs represent one of the most widely diffused prime mover technologies for power generation in the industry thanks also to their simplicity and flexibility. Indeed, simple cycle GTs have the valuable advantages of (i) limited space requirements and reduced specific costs for moderately sized units; (ii) being placed online within minutes for fast start-up and by remote automation, so that only occasional on-site supervision is needed. As a consequence, GT engines are particularly suitable to operate under part-load conditions, to sustain those industrial processes characterized by fluctuating energy demand and also in isolated locations. For instance, GT units are usually employed in the oil and gas sector, in on-shore and off-shore installations, where they are incorporated into the oil refining process or into natural gas compressor stations for

pumping natural gas through pipelines [2]. In addition, GT systems find application also in other areas: industries such as cement, glass, drying, pulp, and paper mills; chemicals production; and tertiary buildings.

The reduction of energy consumption in industry, with the implementation of new and more efficient power generation technologies, are fundamental aspects to meet the new global emission targets and cut process costs [3]. Industries employing simple cycle GTs as prime movers still offer great potential margin for low-cost energy savings and carbon reductions through energy efficiency improvements. Indeed, basic industrial GT engines have limited size, ranging up to 50 MW, with low inherent efficiency, typically not above 40%. A significant amount of fuel energy input is rejected as hot exhaust at relatively high temperatures (400–600 °C) [2]. Figure 1 shows estimated data of heat rejected by many commercial GT units (database of commercial GTs available in Thermoflex software [4] is used) covering the range of size of industrial machines.
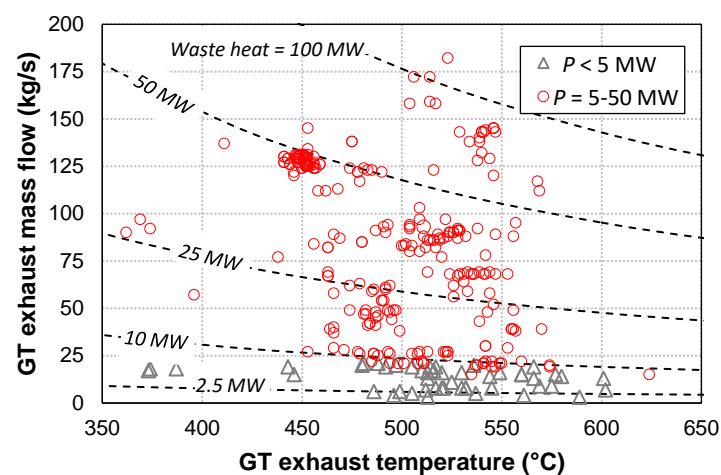
Figure 1. Overview of industrial GT exhaust temperature, air flow, and waste heat ranges calculated at full load conditions, assumed to cool the exhaust gas down to 80 °C.

This wasted energy could be profitably used as a secondary thermal resource in order to increase the efficiency of fuel usage and to mitigate environmental drawbacks. Wasted heat can be firstly utilized to generate additional electric energy to support the industrial process or to be sold to the grid. Moreover, Combined Heat and Power (CHP) solutions, providing steam or hot water for industrial processes, can further improve primary energy utilization, playing a significant role in achieving economic and environmental benefits [5–7].

A well proven Waste Heat Recovery (WHR) solution for large size power plants consists in a steam power plant as the bottomer of the GT. However, small/mid-size industrial GT cannot be always compatible with the traditional steam bottoming cycle featuring complex architecture, especially in industrial applications for which the GT operating conditions often vary following the site demand. More appropriate alternatives might consist in more flexible bottoming cycles, which allow simpler generation of the vapor, thanks to lower critical temperatures of the working fluid. Suitable solutions for the considered operating range are identified in the Organic Rankine Cycle (ORC) and the innovative CO_2 Brayton cycle, or supercritical CO_2 cycle (s-CO_2) [8]; Figure 2 compares the different operating range of heat to power conversion technologies based on bottoming thermodynamic cycles for WHR applications.
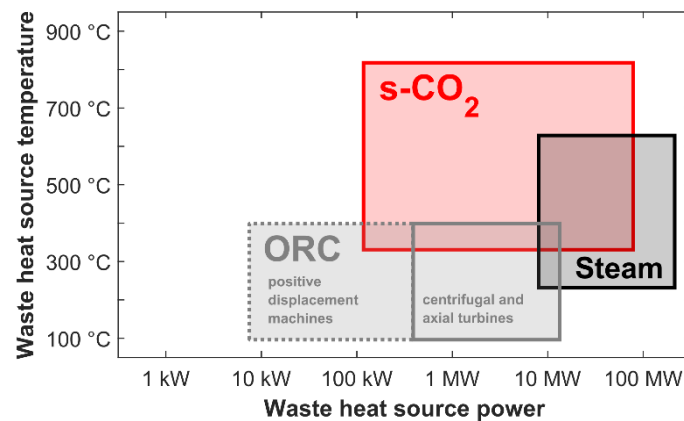
Figure 2. Comparison of different operating range of heat to power conversion technologies based on bottoming thermodynamic cycles for WHR applications (source [8]).

The use of an organic fluid as working fluid, in place of water, introduces several advantages over conventional steam plants for low- to mid-temperature applications [9]: lower fluid specific volume resulting in smaller, more compact, and cheaper equipment; higher condensing pressures (being equal the condensing temperature), reducing turbine size requirements and air-in leakage potential; and dry turbine expansion, avoiding moisture droplets that can cause erosion damage of the turbine blades. More specifically, s-CO_2 technology is competitive with the ORC solution, thanks to its other exclusive features, including high density fluid similar to liquid water throughout the cycle; non-toxic, inexpensive, nonflammable working fluid; and abundant working fluid, possibly provided by greenhouse gas emission sequesters [10].

ORCs are quite diffused in the market and commonly used to generate power in different industrial heat recovery applications with more than 340 MW of installed capacity in the world [11,12]. Many of these applications are WHR from gas turbines, mostly installed on compressor stations along gas pipeline. Important WHR opportunities also come from the cement, metal, and glass industries; nevertheless the ORC installed capacity in these sectors is still scarce compared to its potential [13–16]. The barriers that prevent the growth of this market are, in particular, the lack of green incentives and the long-term paybacks, which determine a high risk on the investment. In addition, industrial capital budgets are limited, and industries usually prefer to give priority to safer investments closer to the company's core business [17].

The s-CO_2 cycle has also long been known, but despite the extensive research carried out in the field, the technology is still at an early stage and not yet ready to be introduced in the market. Current challenges in the s-CO_2 design concern: (i) the development of compact high pressure heat exchangers at reasonable cost, (ii) the reduction of leakage and mechanical losses in turbomachines, and (iii) the optimal regulation and safe operating conditions of the compressor close to the CO_2 critical point [13]. Nowadays, different research programs are being carried out by both industrial and academic research institutes, to develop prototypes of s-CO_2 and study how to overcome these issues. Among them must be mentioned the "EPS100", proposed by Echogen as the first megawatt topping-class commercial-scale supercritical s-CO_2 heat engine, in the phase of validation testing [18], specifically designed for small-scale gas turbines combined cycle (~30 MW total output) applications.

The literature on ORC for industrial WHR applications is extensive; in particular, a detailed investigation of ORC potential as bottomer in an industrial application, comparing several GT models also at part-load operation, is proposed by Bianchi et al. [19]. However, the same does not apply for s-CO_2. The research is still scarce regarding the medium-to-low temperature CO_2 power cycles applications, especially considering industrial GTs as topper cycle. It can be cited the study proposed by Zhou et al. [20], analyzing complex

combined cycle system for off-shore GT WHR, involving s-CO_2 plus a transcritical CO_2 cycle. The analysis is applied to the commercial GT model "Solar TITAN 130", demonstrating promising performance and economic gains for s-CO_2 application in the oil and gas sector.

At present, only few studies are dedicated to comparing ORC and s-CO_2 as industrial WHR solutions. The study of Astolfi et al. [21] compares CO_2 power cycles and ORC, providing thermodynamic performance maps as a function of different heat sources' maximum temperature (200–600 °C) and cooling grades. The authors demonstrated that the most convenient choice sensibly depends on the actual boundary conditions. Yoon et al. [22] compared the off-design performance of ORC and transcritical CO_2 cycle, as the bottoming cycle of a micro gas turbine. They highlight how a CO_2 recuperated cycle can be more performant at part-load operations than a simple ORC. In particular, the CO_2 recuperated cycle exhibits a more efficient heat exchange process at the heat recovery unit, due to the presence of the recuperator. However, a more comprehensive analysis could be performed also including an ORC recuperated configuration.

Except for a few works, the literature lacks studies regarding applications of CO_2-based WHR, in industrial likely operating conditions and specific comparison with its main competitor, the ORC. In a previous work of the authors [23], a preliminary analysis has been performed, comparing s-CO_2 and ORC pure electric and CHP configurations as bottomer of different GT models in design conditions. The additional novel contribution of this work relies on a more systematic investigation on ORC and s-CO_2 potential as energy harvesting technologies inside an industrial facility, employing GT at both full and part-load operation. The performance of ORC and s-CO_2 systems are evaluated as bottoming of selected industrial GT models in CHP configuration. For this purpose, Thermoflex commercial software, providing the GT PRO gas turbine library, has been used for the simulations. The ORC and s-CO_2 systems specifics and costs assumptions have been chosen in line with industrial products and state-of-the-art research experience. A comprehensive analysis has been carried out discussing energy results in terms of electric and thermal power additional production, efficiency, primary energy savings, but also components dimensions, costs, and feasibility. The performance of the whole power plant is evaluated both in design and in part-load operating conditions to account for a realistic load profile.

In comparison to the existing publications, it is the aim of the present work to offer an original contribution in the following aspects:

- The s-CO_2 supercritical cycle is systematically evaluated as bottomer of different GT models for industrial applications, considering realistic operating conditions and part-load operation.
- A comparison between ORC and s-CO_2 power systems performance as industrial WHR solutions is performed. The analysis accounts not only for the thermodynamic cycle but also for the systems specifics and technological limits determined by the state of the art of the technologies.
- An investment cost assessment is proposed for a comprehensive comparison between ORC and s-CO_2 power systems. The influence of the design aspects affecting the investment cost are discussed in detail, highlighting the difference between the compared systems.

The paper is organized as follows: Section 2 describes the analyzed power plant configurations, its specifics, and assumptions made for the simulations; Section 3 explains the adopted modeling approach; Section 4 presents the performance results both in design and at part-load conditions; in Section 5, considerations about component size and investment costs are made; in Section 6, the economic assessment of the bottoming cycles based on the yearly operation is evaluated; and finally Section 7 presents the main conclusions.

2. Power Plant Specifics and Operating Conditions

In this section, the assumptions in terms of analyzed power plant architectures, operating conditions, and imposed technological limits are described. First of all, the whole

plant configuration is presented, then the gas turbines, the s-CO$_2$, and the bottomer cycle selected specifics are discussed in more detail in the dedicated subsections.

2.1. Plant Architecture

The combined heat and power plant comprises the topper gas turbine unit and the bottomer cycle, generating electricity to sustain the electric user and the hot water circuit supplying heat to the thermal user (as schematized in Figure 3). In the considered configuration, the gas turbine exhaust gas is directly conveyed into the heat recovery heat exchanger, here named "GAS HX".

(**a**)
(**b**)
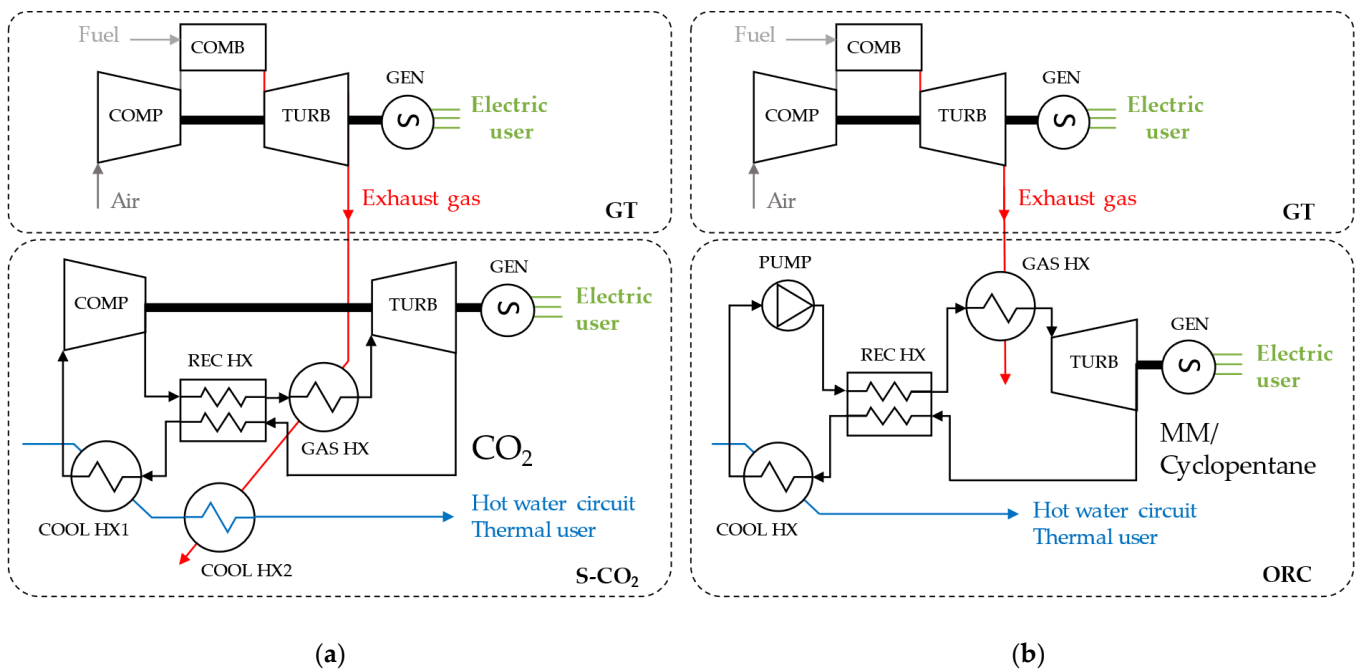
Figure 3. Heat recovery configurations layout: (**a**) s-CO$_2$; (**b**) ORC.

The considered s-CO$_2$ system, represented in Figure 3a, is based on the closed Brayton thermodynamic cycle. In this cycle, the CO$_2$ circulates through the plant being heated into the heat recovery heat exchanger ("GAS HX"), expanded into the turbine, cooled (into the "COOL HX1"), and pressurized by means of a compressor. A simple recuperated cycle is considered as a basic compact and flexible setup. Thus, the efficiency of the s-CO$_2$ is enhanced using an internal heat recuperator ("REC HX"). A generator (GEN) converts the shaft mechanical power into electric power to supply to the electric user. Two heat exchangers employed for cogenerative purpose are present into the plant, named "COOL HX1" and "COOL HX2", recovering heat respectively from the CO$_2$ cooling heat exchanger and from the exhaust gas, downstream of the GAS HX, to supply thermal power to the thermal user hot water circuit.

The ORC subcritical recuperated architecture, represented in Figure 3b, is chosen as comparative bottoming system according to the current state of the art of waste heat recovery applications [8]. In this cycle, an organic fluid circulates through the plant being evaporated and superheated into the heat recovery heat exchanger ("GAS HX"), expanded into the turbine, condensed (into the "COOL HX"), and pressurized by means of a pump. An internal heat recuperator ("REC HX") is used also in this case to improve the cycle efficiency, without over complicating the plant. A generator (GEN) converts the shaft mechanical power into electric power to supply to the electric user, whilst the condenser of the ORC serves as heat exchanger for cogenerative purpose, to supply thermal power to the thermal user hot water circuit.

Before discussing the single systems specifics, some boundary operating conditions concerning the whole power plant operation, are here introduced. These conditions regard: (i) the hot water temperature requested by the thermal user and its return temperature, assumed equal to 90 °C and 25 °C, respectively; (ii) the minimum temperature of the gas turbine exhaust gases at the exhaust stack, limited at 125 °C to avoid the cold-end corrosion issues in the exhaust stack.

Related to these assumptions is the choice of considering two gas heat exchangers for the s-CO_2 configuration, instead of one (see heat exchangers GAS HX and COOL HX2, in Figure 3a). COOL HX2, placed downstream GAS HX, allows to maximize the gas residual heat recovery, by further cooling down the gas until the minimum stack temperature. Indeed, in the s-CO_2 case, it has been observed that a single heat exchanger would not allow to discharge the gas below 250 °C, causing just a partial heat recovery [23]. On the contrary, the GAS HX of the ORC solution has proved to be more performant, as discussed in more detail in the results section.

2.2. Industrial Gas Turbines Specifics

A variety of gas turbine models with different size are employed in industrial applications. Small and mid-size machines (MW size range) are used in flexible multiple arrangements, installed on board of small production facilities, usually operating at part-load conditions, e.g., in off-shore plants. Larger power rating units (ranging up to tens of MW), both heavy-duty and aeroderivative machines, are preferred instead on larger facilities requiring higher power needs and working under more stable conditions. Thus, to perform a systematic analysis, four different types of commercial gas turbines, in terms of size and regulation strategy, are investigated; in particular, gas turbine models often used in the oil and gas sector are considered [19,24].

The design data of selected GT units are summarized in Table 1. These gas turbine models are characterized by sizes ranging between 1 and 30 MW, with efficiency values increasing with the size, from 24% for Kawasaki GPB15 up to 36% for Siemens GT 700 machine. Important variables to also consider are the temperature and the flow rate of the exhaust gases, which affect the amount of energy that can be recovered by the bottomer power cycle. In particular, exhaust gas mass flow rate raises with the gas turbine size and it ranges between 8 and 89 kg/s for the selected gas turbines. Exhaust gas temperature is centered around 500–550 °C, varying between 474 and 574 °C.

Table 1. Selected gas turbines nominal data.

	Kawasaki GPB15 (GT1)	GE5 (GT2)	Solar Titan 130 (GT3)	Siemens GT 700 (GT4)
Output power (MW)	1.5	5.5	15	30
Turbine inlet temperature (°C)	991	1232	1093	1260
Pressure ratio (-)	9.4	14.8	15.7	17.6
Efficiency (%)	24.2	30.6	33.3	36
Exhaust flow rate (kg/s)	8	19	49	89
Exhaust temperature (°C)	520	574	474	518
Regulation strategy	VTIT	VIGV	VTIT	VSS

These values can significantly vary at part-load conditions, strongly influencing the bottoming cycle performance.

Figure 4 reports manufacturer data provided by the GT PRO gas turbine library [4], showing how the exhaust flow rates and temperatures values vary with the gas turbine load for the different models; it can be observed that different gas turbine regulation strategies determine different trends. Three kinds of regulation strategies can be distinguished, here named VTIT (variable turbine inlet temperature), VIGV (variable inlet guide vanes), and VSS (variable shaft speed), which consist of:

- VTIT—variable amount of fuel injected in the combustor into a constant air mass flow rate; hence, regulating the air–fuel ratio and so the turbine inlet temperature. This leads to exhaust temperatures, which decrease as the gas turbine load (GT load) decrease, whilst the exhaust flow rate remains almost constant. GT1 and GT3 are examples of gas turbines regulated by means of the VTIT control.
- VIGV—variable compressor geometry resulting in a variable air mass flow. This kind of regulation strategy allows to work at part-load conditions without decreasing the operating temperatures, whilst the mass flow rate decreases with the load. GT2 is an example of gas turbine regulated by means of the VIGV control.
- VSS—variable shaft speed at the gas generator in multi-shaft engines. This is the strategy that allows for the most limited reduction in shaft efficiency at part-load conditions, compared to the other strategies. A decrease in both the exhaust temperature and flow rate occurs in this case. GT4 is an example of gas turbine regulated with the VSS control strategy.
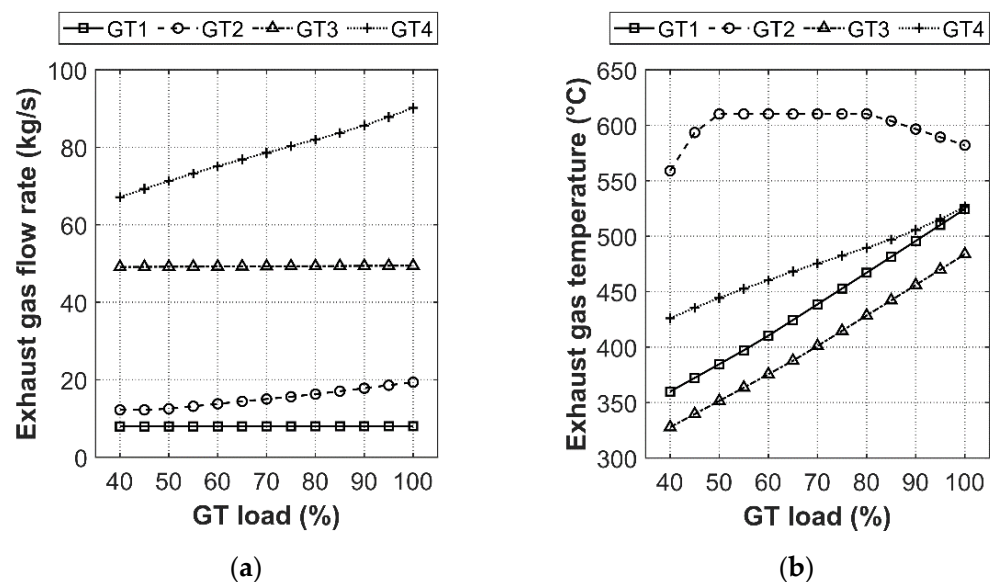

Figure 4. Gas turbines' part-load operation: (**a**) exhaust gas flow rate; (**b**) exhaust gas temperature.

2.3. Supercritical CO_2 Cycle and ORC Specifics

The choice of the s-CO_2 component specifics and boundary operating conditions, as shown in Table 2, are derived from a literature survey based on different studies and experimental data [20,22,25,26]. The compressor minimum inlet temperature and pressure are imposed respectively equal to 35 °C and 75 bar. This choice grants maintaining supercritical conditions all along the cycle, given CO_2 temperature equal to 31 °C and critical pressure equal to 74 bar. In line with the current research data, the cycle maximum pressure is limited to 300 bar because of technological limits. The turbine and the compressor isentropic efficiencies values are considered different for s-CO_2 power plant size lower or higher than 3 MW to account for the machine size-effect over the performance. The recuperator thermal effectiveness minimum pinch point assumed for the heat exchangers, pressure drops, and heat loss values are also reported in Table 2, and are chosen equal for the ORC and the s-CO_2 systems for a fair comparison between the two systems.

Table 2. Bottomer cycles design specifics.

Size	s-CO$_2$		ORC	
	<3 MW	**>3 MW**	**<3 MW**	**>3 MW**
Fluid	Carbon Dioxide		MM	Cyclopentane
Low pressure	75 bar		0.9 bar	3.7 bar
High pressure upper limit	300 bar		17 bar	40 bar
Turbine isentropic efficiency	85%	90%	80%	85%
Op. machine isentropic efficiency	70%	80%		60%
Recuperator thermal effectiveness		80%		
Pressure drop across heat exchangers		1%		
Heat exchangers normalized heat loss		1%		
Heat exchangers minimum pinch point		5 °C		
Other limits	Min. temperature = 35 °C (supercritical threshold)		Max. temperature = 280 °C (stability limit)	

The ORC components specifics and boundary operating conditions are selected as consistent with existing industrial established products [19] (see Table 2). The first design decision concerns the choice of the working fluid. Cyclopentane and hexamethyldisiloxane (MM) (respectively belonging to the hydrocarbon and the siloxane families) are the selected fluids since they are state-of-the-art organic fluid in industrial medium waste heat recovery application [19]. Fluids belonging to the hydrocarbon and siloxane families are demonstrated to be the most suitable fluids for the medium temperature applications, thanks to their quite high critical temperature. Indeed, a value of the critical temperature quite similar or slightly higher than the target evaporation temperature is suggested to simultaneously achieve good thermal matching between fluids and exhaust gas and to avoid excessively low vapor densities, which lead to increasing system cost. Cyclopentane and MM feature similar critical temperature and thermal stability limits, while they appreciably differ in terms of critical pressure and molecular weight. In particular, MM presents a higher molecular weight, which leads to lower speed of sound during the expansion, allowing to design the turbine with a lower number of stages (even only a single stage). This is the main reason why MM is the ideal candidate for small size applications (ORC size < 3 MW), even if, on the other hand, due to its high molecular weight, MM also presents smaller enthalpy drop and expansion specific works if compared to cyclopentane.

The operating conditions bounded by the selection of a working fluid rather than another are the cycle maximum temperature and the evaporating and condensing pressure values. In more detail, the temperature is conservatively limited to 280 °C to not overcome thermal stability limit corresponding to 300 °C. The cycle maximum pressure (corresponding to the evaporating pressure) is limited to the 90% of the critical pressure value (equal to 45.1 bar for the cyclopentane and 19.4 bar for the MM). The condensing pressure instead mainly depends on the cooling medium temperature. Its value can be considered as a first approximation equal to the fluid saturation pressure value at the cooling medium temperature (see Figure 5a). In this case also, the turbine and the pump isentropic efficiencies values are considered different for ORC power plant size lower or higher than 3 MW, to account for the machine size-effect over the performance.

Fluids thermodynamic properties useful for the analysis are reported in Figure 5; where the saturation pressure and density are plotted against temperature.
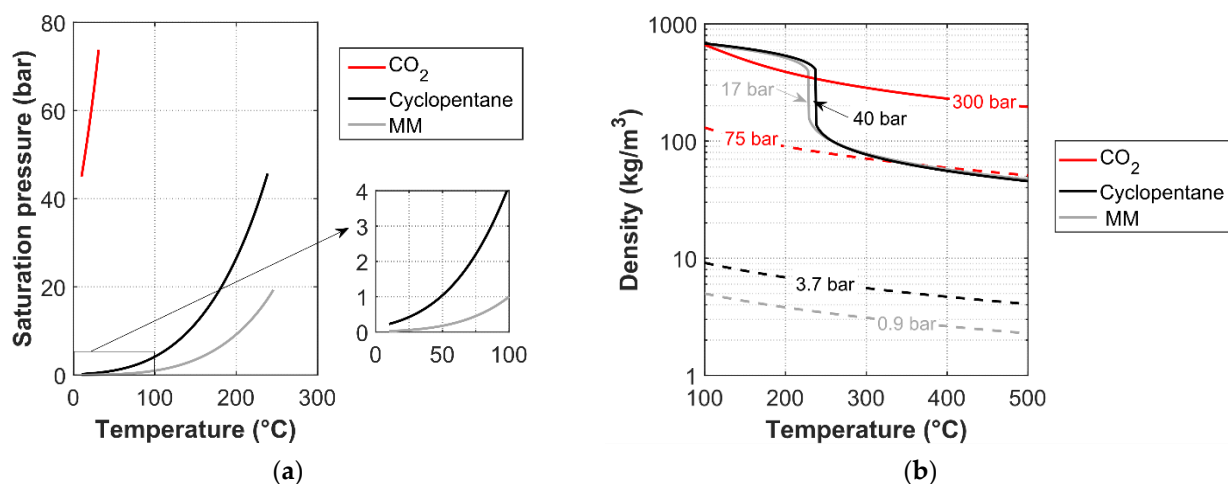
Figure 5. Fluid thermodynamic properties: (**a**) saturation pressure; (**b**) density (calculated with Refprop [27]).

3. Modeling Approach

Thermoflex commercial software [4] was used to simulate the whole combined power plant, involving both the gas turbine unit and the bottoming cycle, i.e., the s-CO_2 or the ORC system. Thermoflex is software dedicated to designing complex power plants, which relies on a built-in library of components modeled on the base of a lumped parameters approach. By following three consecutive steps, namely "Thermodynamic design", "Engineering design", and "Off-design", the software allows for the simulation of the energy systems performance both in design and off-design operation. In the first step, "Thermodynamic design", the software solves preliminary energy and mass balances to evaluate the plant thermodynamic performance. In the second step, the "Engineering design", the size and the geometry details of each components is established, on the basis of the imposed design boundary conditions and components specifics. Finally, in the "Off-design" step, being defined the design characteristics of single components, it is possible to evaluate the plant performance in operating conditions different from the design ones.

The approach used to model the single components of the plant at part-load conditions is described below:

- The gas turbine unit is modeled as a single component by means of a black box approach. This component can simulate a wide choice of commercial gas turbine models that are featured in the GT PRO gas turbine library, accounting for design data and performance maps directly supplied by the manufacturers. The bottomer cycle instead is modeled by connecting the single components that constitute it: i.e., the heat exchangers, turbine, condenser, and operating machine. In this case, some inputs defining the components performance must be imposed by the user. Specific component inputs are summarized in Table 2.

- The heat exchangers' off-design behavior is described by the so called "thermal resistance scaling" method. Following this method, the design point convective heat transfer coefficients (UA_{des}) of the generic fluid involved in the heat exchange, is scaled as function of the ratio between the actual mass flow rate, $\dot{m}$, and the one calculated in the design point, $\dot{m}_{des}$. A scaling exponent equal to 0.8 (which recalls the exponent for the Reynolds number in the Dittus Boelter correlation) is applied to the mass flow rate ratio. This approach is valid since the thermal–hydraulic properties of the fluids do not change much over the range of considered conditions, and the fluid velocity remains the main parameter affecting the heat transfer coefficients.

$$UA = UA_{des} \times \left(\frac{\dot{m}}{\dot{m}_{des}}\right)^{0.8} \tag{1}$$

It can be pointed out that in conditions of fluid phase change or in proximity of the critical pressure, the program implement a discretization of the heat exchanger for the determination of the heat exchanger's UA, automatically assigning distinct zones for each phase of the fluid, or if the pressure is near the critical pressure, 13 equally weighted zones are assumed. Normalized heat loss in the heat exchangers is computed as a percentage, relative to the heat transferred out of the higher temperature fluid. The pressure drops across the heat exchangers, Δp, is obtained by means of Equation (2), expressing the relationship between the flow resistance coefficient μ (initialized in the design-point), the pressure drops, the mass flow rate $\dot{m}$, a dimensional constant C, and the average specific volume v (mean between the specific volumes at the inlet and at the outlet).

$$\mu = \frac{\Delta p}{v \times \dot{m}^2 \times C} \tag{2}$$

- The turbine inlet conditions, in terms of temperature and flow rate, vary at part-load operation depending on the exhaust gas temperature and flow rate values. The turbine inlet temperature, T, is kept equal to its maximum possible value, respecting the constraints related to the GAS HX performance and the fluid thermal stability limit. The off-design inlet pressure, p, is determined consequently by assuming the "sliding pressure" part-load control. Following this regulation strategy, the pressure at the turbine nozzle inlet vary proportionally to the mass flow rate, $\dot{m}$, in order to keep constant the flow function parameter value, FF, assuming chocking conditions.

$$FF = \frac{\dot{m} \times \sqrt{T}}{p} = \text{const} \tag{3}$$

However, there are situations in which it is not possible to maintain constant the flow function parameter, as happens for example when the fluid temperature at the expander inlet changes significantly. In this case, the turbine isentropic efficiency, η_{is}, is reduced with respect to its full load value, $\eta_{is,des}$, based on the flow function, as follow:

$$\eta_{is} = \eta_{is,des} - \frac{\left(\dot{m} \times \sqrt{v/p}\right)_{des}}{\dot{m} \times \sqrt{v/p}} \tag{4}$$

4. Performance Results

4.1. Design

In this section, the s-CO_2 and the ORC configurations are compared in their design operation as bottoming cycles of the four different selected gas turbines. Indexes analyzed in this section are (as defined in Table 3): (i) the heat recovery effectiveness, ε, (ii) the bottoming cycle efficiency, η_{bott}, (iii) the relative, λ, and absolute bottoming power production, $P_{net,bott}$, (iv) the plant efficiency, η and τ and primary energy savings, PES.

Table 3. Performance indexes for design performance evaluation.

| Index	Equation
Heat recovery effectiveness	$\varepsilon = Q_{rec}/Q_{ava} = \frac{Q_{GAS\ HX}}{\dot{m}_{ex} \times c_{p,ex} \times (T_{ex} - T_{amb})}$
Bottoming cycle efficiency	$\eta_{bott} = P_{net,bott}/Q_{GAS\ HX}$
Relative bottoming power production	$\lambda = P_{net,bott}/P_{GT}$
Bottomer expander power	P_{exp}, with $P_{net,bott} = P_{exp} - P_{op.\ machine}$
Electric efficiency	$\eta = \frac{P_{net,bott} + P_{GT}}{F}$
Thermal efficiency	$\tau = \frac{Q_{cog}}{F}$, with $Q_{cog} =$ $\begin{cases} Q_{COOL\ HX1} + Q_{COOL\ HX2} & , \ if\ s-CO_2 \\ Q_{COOL\ HX} & , \ if\ ORC \end{cases}$
Primary energy saving	$PES = 1 - \frac{1}{\frac{\eta}{\eta_{ref}} + \frac{\tau}{\tau_{ref}}}$, with $\eta_{ref} = 52.5\%$ and $\tau_{ref} = 90\%$ (source [28])

Figure 6a indicates that the ORC system can recover a higher amount of thermal power at the heat recovery heat exchanger ("GAS HX"), showing higher heat recovery efficiency, slightly increasing with the gas turbine size (GT size). The better heat recovery performance of the ORC is also due to the heat transfer coefficients of the MM and cyclopentane compared to the CO_2 cases, especially given by the fluid phase change inside the evaporator. As anticipated in Section 2, because of the better heat recovery performance of the ORC, this configuration is able to fully exploit the exhaust gases' residual heat by means of a single heat recovery heat exchanger. On the contrary, for the s-CO_2 case, it has been observed that a single heat exchanger would not allow to discharge the gas below 250 °C, causing just a partial heat recovery. From these considerations comes the choice of considering two gas heat exchangers for the s-CO_2 configuration, instead of one (see heat exchangers GAS HX and COOL HX2, in Figure 3a), with the aim of further exploiting the exhaust residual heat to provide additional thermal power to the cogenerative thermal user.
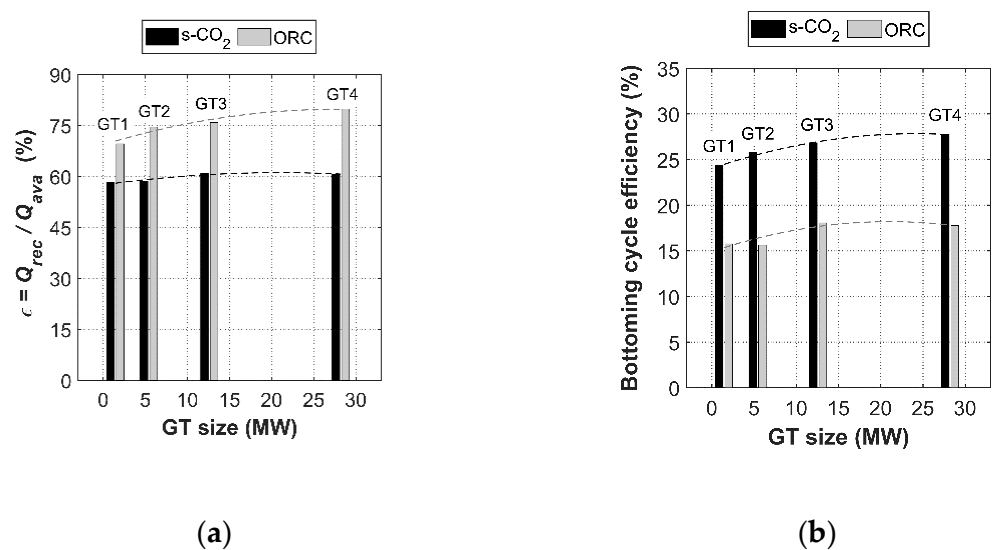
Figure 6. Bottoming cycles design performance: (**a**) heat recovery efficiency; (**b**) bottoming cycle efficiency.

Despite the ORC presenting higher heat recovery efficiency, the s-CO_2 is demonstrated to better exploit the recovered thermal power, showing higher bottoming cycle efficiency, up to the 28% (see Figure 6b). The ORC efficiency instead does not exceed the 18%. In general, the bottoming cycle efficiency increases with the GT size and the thermal power available with the exhaust gas. More specifically, some considerations can be made about the bottoming cycles' performance in combined heat and power application and the influence of the thermal user requested temperature. It is observed that the ORC expander enthalpy drop (thus, the specific work) can be considerably affected by the condensing temperature, which determine the condensing pressure and the expander pressure ratio, consequently. This is not valid instead for the s-CO_2 pressure ratio, which does not depend on the thermal user requested temperature. This explains the not excellent ORC electric production performance [23].

The bottoming cycle power production depends on both the heat recovery efficiency and the cycle efficiency and, more specifically, the product between the two. Figure 7 presents the bottoming cycle design performance in terms of actual power production, showing that the s-CO_2 is the system that exhibits a higher electric power production under the same topper gas turbine. The s-CO_2 allows generating, on average, 31% of the power produced by topper gas turbine, whilst the ORC, 25% (see Figure 7a). The relative bottoming power production decreases with the gas turbine size, caused by the increase of the gas turbine efficiency, which leads to a decrease of the relative rejected heat.
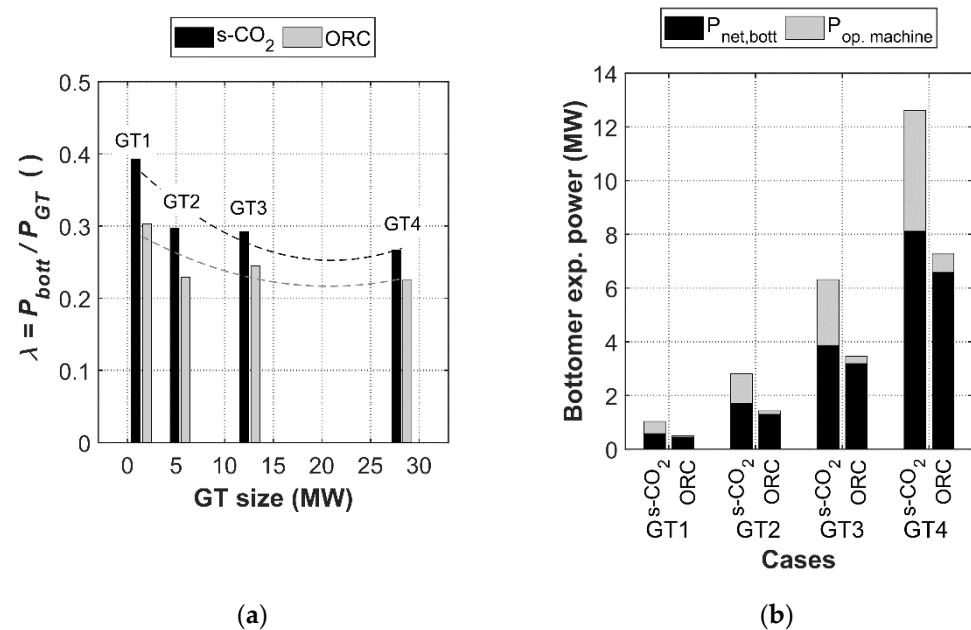
Figure 7. Bottoming cycles' design performance: (**a**) relative and (**b**) absolute bottoming power production.

The absolute net bottomer power production ranges between 578–81,117 kW and 447–6580 kW, for the s-CO_2 and the ORC, respectively (see Figure 7b), increasing with the GT size. An interesting point to take into consideration is the amount of power required by the operating machine to sustain the bottoming cycle, and its weight on the expander power production, equal on average to 40% for the s-CO_2 and to 9% for the ORC. This point indeed may not be determinant on the energetic performance, but it can be when evaluating the economic aspect, as discussed in the economic results section.

To comprehensively evaluate the electric and thermal performance of the whole power plant, the PES index is plotted on the electric and thermal efficiency cartesian plane in Figure 8. The electrical efficiency increases with the GT size ranging between the 35% and the 45%. It means that the plant electric efficiency increments with respect to the gas turbine efficiency only, on average of 8.7 percentage points with the s-CO_2 and of 7.0 percentage points with the ORC bottoming system. On the other hand, the thermal efficiency generally decreases by increasing the GT size, due to the consequent decreasing relative discharged heat. The thermal efficiency is limited in a narrow range centered around the 36% for the ORC solution, whilst it varies more for the s-CO_2 case, ranging between the 37% and the 44%. The corresponding PES values are increasing with the GT size and largely positive in many cases (up to 22% for GT4 with s-CO_2 cycle). The achievable primary energy savings are attractive in most of the cases. Only in case of GT1 does the ORC bottomer becomes less attractive, showing PES close to 0.

4.2. Part-Loads

In this section the part-load performance of the bottoming cycles is analyzed as a function of the GT load, varying between its technical minimum, assumed equal to 40%, and full load. The trends of the bottoming cycle produced electric and thermal power, normalized on their design values, are reported in Figure 9. The normalized values are useful to immediately compare the effect of the gas turbines regulation strategy on the bottoming cycles' part-load performance.
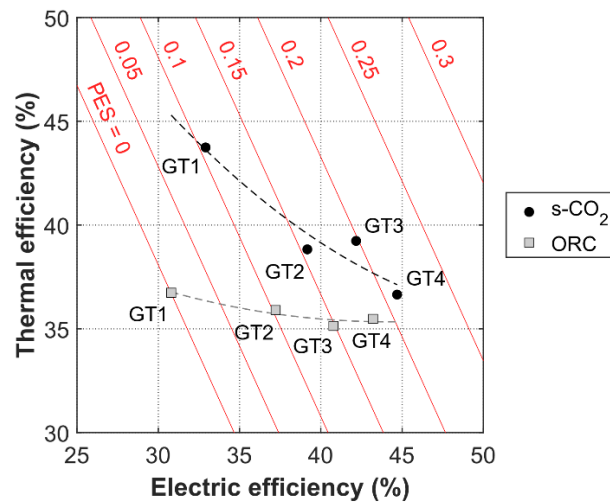
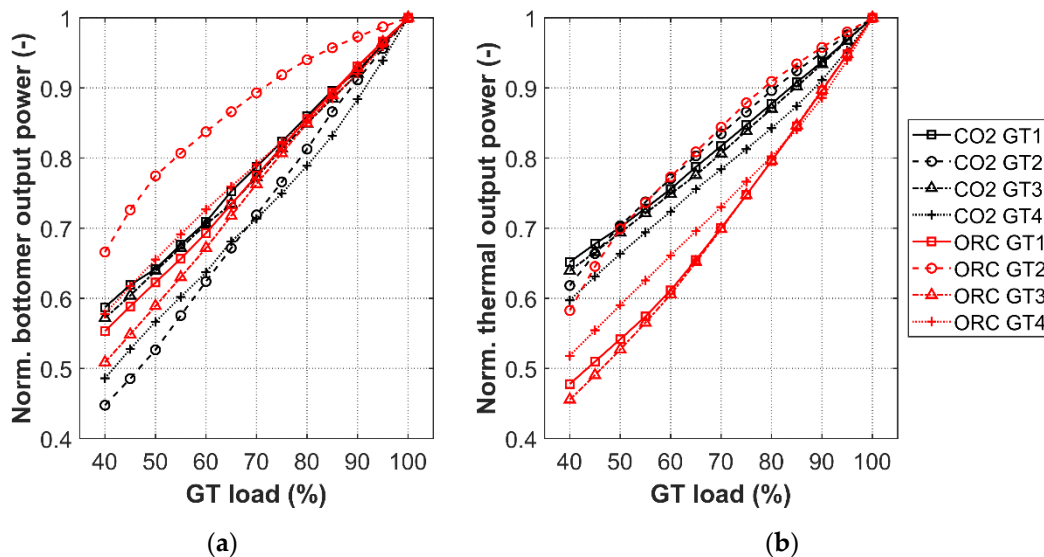**Figure 8.** Plant design thermal end electric efficiency. Lines at constant PES values are traced in red.

(**a**)

(**b**)

Figure 9. Bottoming cycles' part-load performance: (**a**) electric power output and (**b**) thermal power output, normalized to their design values.

Focusing on the electric production (see Figure 9a), it can be observed that the s-CO_2 system maintains higher part-load performance when working with GT1 and GT3 turbines regulated by means of the VTIT strategy; thus, working with almost constant exhaust flow rate (see Figure 4a). On the contrary, the ORC power plant results to be more performant when working with GT2, and following GT4, GT1, and GT3, thus benefitting from working with exhaust temperatures that do not change significantly with respect to the design values (see Figure 4b).

The same considerations apply to the thermal power production at part-load conditions (see Figure 9b). It can be also observed that a higher performance derating occurs for the ORC configuration with respect to the s-CO_2, except for the GT2 case, which is instead in line with the s-CO_2 curves.

5. Components Size and Investment Considerations

Besides performance considerations, it may be also important to take into account some design aspects affecting the investment cost and the system footprint. In this section, different size indexes are introduced as necessary to estimate the component investment

costs, by means of chosen cost correlations. Then, the size and investment results are discussed.

5.1. Indexes and Correlations

The size indexes comprise the heat exchangers global heat transfer coefficient, UA, and the turbine size parameter, SP. The first depends on the heat exchanger exchanged power, Q, and its mean logarithmic temperature difference, ΔT_{ml}; see Equation (5). The second is defined as the ratio between the fluid volume flow rate evaluated at the expander outlet pressure, and the isentropic enthalpy drop trough the expander, Δh_{is}; where the volume flow rate is given by the ratio between the fluid mass flow rate, $\dot{m}$, and its density, $\rho_{out,is}$, see Equation (6). Thermodynamic properties of the working fluid are calculated by means of the Refprop thermodynamic library [27].

$$UA = \frac{Q}{\Delta T_{ml}} \tag{5}$$

$$SP = \frac{\left(\dot{m}/\rho_{out,is}\right)^{0.5}}{\Delta h_{is}^{0.25}} \tag{6}$$

The generic formula to evaluate the i-th component investment cost, C_i, is based on re-scaling a reference cost value, C_{ref}, by the ratio between the actual component size, $size_i$, and its reference size value, $size_{\text{ref}}$ [29]. An exponent, n, is usually applied to the scaling factor and the effect of some operating conditions can be accounted by applying some correction factors, $corr$, see Equation (7). In this analysis, the correlation parameters (as reported in Table 4) come from literature works providing data from s-CO_2 and ORC and specific components vendors (respectively [30,31]).

$$C_i = C_{ref}\left(\frac{size_i}{size_{ref}}\right)^n \times corr \tag{7}$$

Table 4. Cost correlations.

	Component	C_{ref} Value	Size Parameter	Size$_{\text{ref}}$ Value	n	corr
	Turbine	149,732 EUR *	P_{exp}	1 MW	0.5561	/
	Compressor	1,008,600 EUR *	$P_{op.\ machine}$	1 MW	0.3992	/
s-CO₂ [30]	GAS HX	40.55 EUR *	$UA_{GAS\ HX}$	1 W/K	0.7544	/
	REC HX	40.55 EUR *	$UA_{REC\ HX}$	1 W/K	0.7544	/
	COOL HX1,2	26.96 EUR *	$UA_{COOL\ HX}$	1 W/K	0.75	/
	Turbine	1,230,000 EUR	SP	0.18 m	1.1	/
	Pump	14,000 EUR	$P_{op.\ machine}$	200 kW	0.67	/
ORC [31]	GAS HX	1,500,000 EUR	$UA_{GAS\ HX}$	4000 kW/K	0.9	$f(p_{max})$
	REC HX	260,000 EUR	$UA_{REC\ HX}$	650 kW/K	0.9	$f(p_{max})$
	COOL HX	530,000 EUR	$A_{COOL\ HX}$	3563 m²	0.9	/

* Values converted from original values in US dollar.

5.2. Results Discussion

The computed values of the heat exchangers global heat transfer coefficients and the turbine size parameter are reported in Figure 10. Figure 10a shows the total heat exchanger size (expressed in terms of UA) and its distribution between the different heat exchange sections, "GAS, HX", "REC, HX", and "COOL, HX". From Figure 10a, it can be observed that the total heat exchanger size is similarly divided among the various heat exchange sections, varying the examined gas turbine for a given bottoming cycle solution, whilst the $UA_{rec,HX}$ value is similar between the s-CO_2 and the ORC solutions, suggesting similar internal heat recovery conditions, and $UA_{gas,HX}$ and $UA_{cool,\ HX}$ can greatly differ. s-CO_2 $UA_{gas,HX}$ is on average 9 times the ORC $UA_{gas,HX}$, mainly because of the higher

convective heat transfer coefficient of cyclopentane/MM into the evaporator, also due to the fluid phase change, which guarantees a more performant heat exchange. Concerning instead "COOL HX" (comprehending both "COOL HX1" and "COOL HX2" for the s-CO$_2$), $UA_{cool,HX}$ values are more similar between the different configurations. However, a slight increase in the size parameter is observed when using the ORC rather than the s-CO$_2$ solution, indicating worse matching between the working fluid heat exchange profile and that of the cold source. This analysis suggests that higher heat exchanger investment costs can be expected if installing s-CO$_2$ bottoming cycle rather than ORC, given the higher total heat exchanger size, which can be more than 3 times the ORC configuration's one.

(**a**)   (**b**)
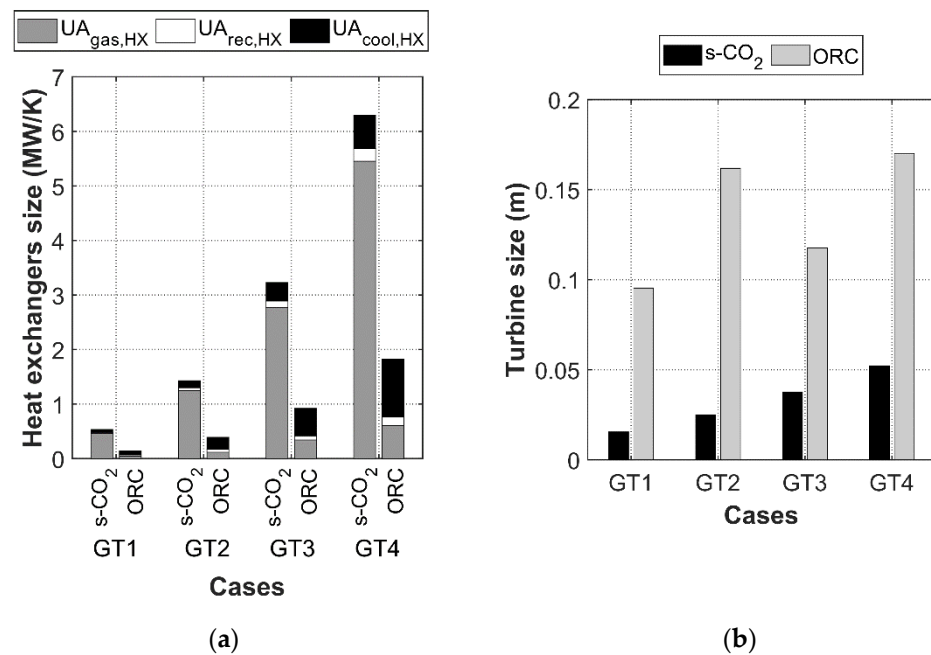
Figure 10. Component size: (**a**) turbine size parameter; (**b**) heat exchangers' global heat transfer coefficients.

Opposite conclusions can be drawn from the turbine size parameter analysis. Focusing on Figure 10b, it can be observed that comparing the different bottoming cycle options, the s-CO$_2$ exhibits lower turbine size parameter values, mainly due to the higher density of the fluid passing through the expander. Indeed, the s-CO$_2$ cycle works at high pressures, between 300 and 75 bar, corresponding to relatively high CO$_2$ density values that range between 700 and 60 kg/m^3. Cyclopentane and MM, instead, both expand in ORC at lower pressure and lower density (below 10 kg/m^3), leading to less compact expander machines (see Figure 5b).

The investment cost results reflect the considerations made about the components size. Figure 11 shows that the s-CO$_2$ requires significantly higher heat exchanger costs because of the large size of the GAS HX but also the high investment cost still associated to this component, due to the current challenges related to the structure design and the selection of materials compatible with the high cycle pressures and the strong corrosive behavior that CO$_2$ shows at high temperatures [32]. The s-CO$_2$ also requires larger size (see Figure 7b) and more expensive operating machines. On the other hand, the ORC operates with larger turbines, which entail higher expander investment costs. In the view of the above, the total investment cost, given by the sum of the single component costs, result in being fairly higher for the s-CO$_2$ rather than for the ORC, despite the s-CO$_2$ present both better electric and thermal performance (as discussed in Section 4).
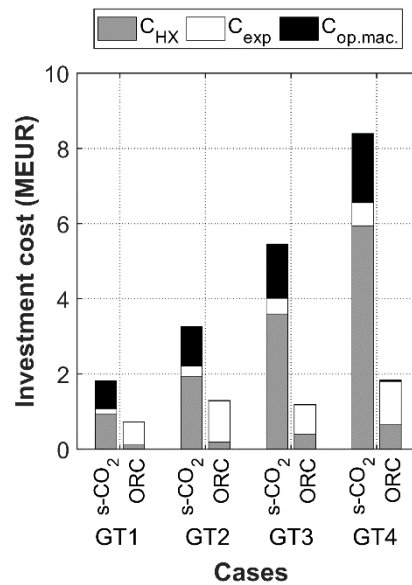
Figure 11. Investment cost.

6. Yearly Operation and Economic Assessment

A yearly demand profile of a natural gas compressor station is considered here as reference case study to evaluate the yearly energetic production of the proposed bottoming cycles, namely the s-CO_2 and the ORC, and their feasibility. In first analysis, an average carbon tax value is assumed for the reference case. Then, the investment is evaluated by considering also more favorable economic conditions, i.e., a full load yearly demand profile and a higher carbon tax value.

6.1. Economic Indexes

The return on the investment is estimated by assuming that introducing the bottoming cycle produces a fuel saving as it would cover the energy demand that otherwise should be provided by another energetic system. This primary energy saving, E_{PES}, is computed as follows, considering both the electric, $E_{net,bott}$, and the thermal energy production, E_{cog}, in a year:

$$E_{PES} = \frac{E_{net,bott}}{\eta_{ref}} + \frac{E_{cog}}{\tau_{ref}} \tag{8}$$

The reduction of the fuel consumption is reflected in reduced greenhouse gas emissions and in reduced plant operation costs. The differential net present value has been calculated according to Equation (9), where CF_i is the differential cash flow at the i-th year corresponding to the yearly avoided costs, q is the discount rate assumed equal to 6%, I is the total investment, and PB is the payback period considered equal to 20 years.

$$\Delta NPV = \sum_{i=1}^{PB} \frac{CF_i}{(1+q)^i} - I \tag{9}$$

The avoided costs include the fuel purchasing reduction and the CO_2 emission avoided cost. The cost due to the fuel consumption is function of the fuel saving and its specific cost per unit of primary energy, C_{fuel}. The cost due to the CO_2 emissions is computed as the product between the avoided mass and its specific cost, C_{CO2}. It is assumed that the avoided CO_2 amount is equal the CO_2 mass that would be produced by the stoichiometric combustion of the fuel saved, assumed to be natural gas (thus, the fraction of carbon, x_C, is

likely considered equal to 0.75 and the lower heating value, *LHV*, is considered equal to 47 MJ/kg [33]).

$$CF_i = E_{PES} \times \left(C_{fuel} + \frac{44}{12} \times \frac{x_C}{LHV} \times C_{CO2} \right) \tag{10}$$

C_{fuel} is chosen equal to the average natural gas price in Europe in 2019, 26.7 EUR/MWh [34], and a reference carbon tax value is selected equal to 40 EUR/ton, as in line with its average value in some European countries [35].

6.2. Reference Case Results

In the reference case, the gas turbine load profile of a natural gas compressor station [36] is considered. The number of operating hours (on the yearly base) in which the gas turbine works at given GT load are presented in Figure 12. It is shown that the gas turbine works at full load for about half of the operating hours, whilst for the rest of the time, the GT load is almost equally distributed between the 50% and the 90%.
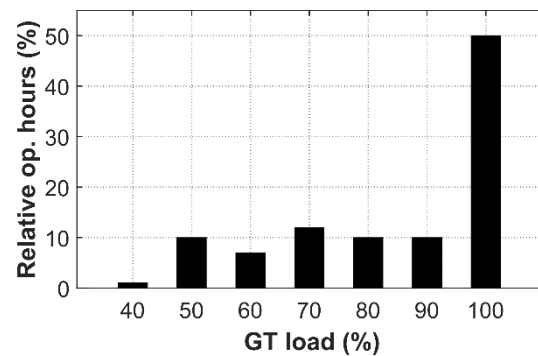

Figure 12. Reference yearly demand profile of a natural gas compressor station (source [36]).

A summary of the design performance results, the yearly energy production and savings, is reported in tabular form (see Table 5). As discussed in the previous sections, the s-CO$_2$ configurations exhibit better performance than the ORC, in design operation, both concerning the electric and the thermal production. The yearly energetic results demonstrate that this applies also to the yearly based performance; indeed, the s-CO$_2$ allows saving, on average, 16% more fuel than the ORC solution and consequently also 16% more CO$_2$ emissions. The same increase is observed for the yearly economic gain.

Table 5. Results summary.

	GT1		GT2		GT3		GT4	
	s-CO$_2$	ORC	s-CO$_2$	ORC	s-CO$_2$	ORC	s-CO$_2$	ORC
Bottomer size (MW)	0.58	0.45	1.70	1.30	3.86	3.19	8.11	6.58
Electric power output (MW)	2	1.87	7.02	6.65	16.25	15.66	35.73	34.54
Thermal power (MW)	2.65	2.23	6.94	6.42	15.07	13.49	29.30	28.36
Electric energy (GWh/year)	15.32	14.43	54.36	51.95	124.81	120.69	274.38	266.89
Thermal energy (GWh/year)	21.47	17.12	56.55	52.46	121.52	103.57	233.24	220.31
Fuel saving (GWh/year)	32.19	25.64	87.63	78.45	189.62	161.75	371.16	342.37
Avoided emissions (tonCO$_2$)	1.88	1.50	5.13	4.59	11.09	9.46	21.72	20.03
Economic gain (kEUR/year) *	75.33	60.01	205.09	183.61	443.80	378.57	868.68	801.30

* Reference case results—Figure 12 demand profile and C_{CO2} = 40 EUR/ton

Yet, in spite of the significant economic gain expected from the s-CO$_2$ operation, the net present value of the investment does not seems to always be favorable on this system, as shown in Figure 13 (see "s-CO$_2$ ref" and "ORC ref" data). This is mainly due to the fact of the still high investment costs associated with this fledgling technology, in particular

concerning the recovery heat exchangers. However, given the considerable economic gain, it is not excluded that once the technology becomes established, s-CO$_2$ may become a very competitive solution for industrial gas turbines' heat recovery. On the other hand, the current lower investment costs required to install an ORC system make this solution practical and often profitable.
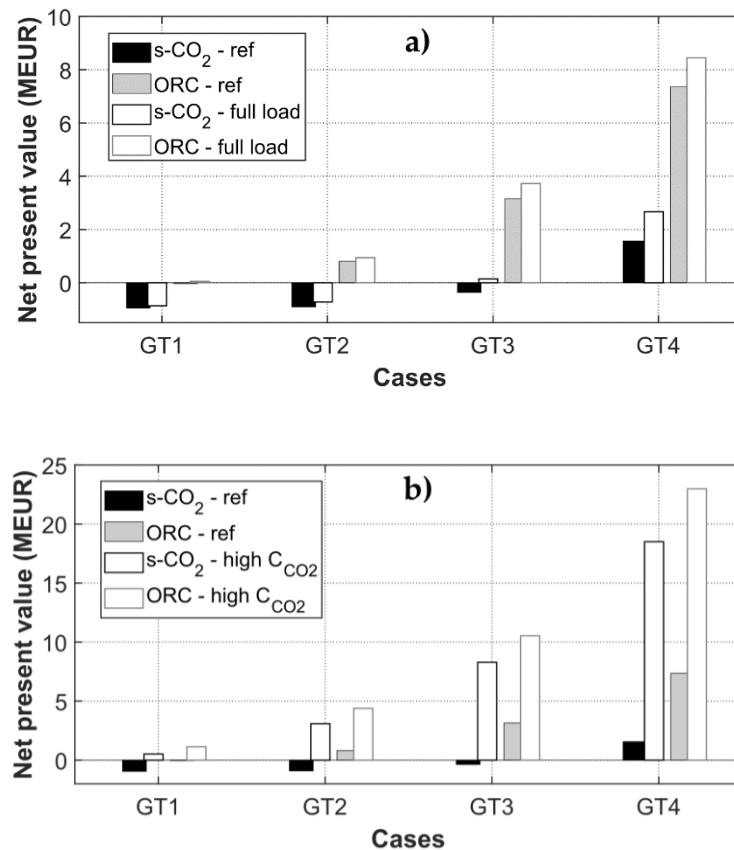
Figure 13. Net present value comparison between the reference case study and: (**a**) a full load yearly operation and (**b**) the application of a higher carbon tax.

6.3. Costs Parametric Analysis

Factors that can influence the bottoming cycles' feasibility, and which can considerably vary from application to application, are the user profile demand and the carbon tax value. The profile demand can be more or less shifted to high or low loads, whilst the carbon tax value is variable from country to country can be null or even equal to 108 EUR/ton, as in the case of Sweden [35]. Thus, to complete the economic analysis, the investment is evaluated by considering also more favorable economic conditions, i.e., a full load yearly demand profile (see Figure 13a) and a higher carbon tax value, equal to 108 EUR/ton (see Figure 13b).

These results reveal that among the two analyzed factors, the most decisive one on the return of the investment is surely the carbon tax value. It is observed, indeed, that higher values of the carbon tax reduce the gap between the gain obtained with the ORC and the one obtained with the s-CO$_2$ (see Figure 13b). This is due to the higher valorization of the avoid emissions, which are the 15% higher for the s-CO$_2$ than for the ORC (see Table 1). Generally, with higher values of the carbon tax, the s-CO$_2$ system may become convenient as the bottomer of all the analyzed gas turbines, as well as the ORC, with a net present value more than twice of its reference value.

The return on the investment is instead less sensitive to the variation of the profile demand (see Figure 13a). Working at full load during the entire year does not grant such a significant gain equal to the one obtainable by introducing a high carbon tax. Comparing

the case at the reference load profile and the full load profile, the net present value increase of the 17%. However, in some cases, the yearly demand profile can be decisive to have a return on the investment, for example, when the investment is uncertain and the net present value is near to zero. This is the case of the GT1-ORC and the GT3 s-CO_2 configurations, which are not convenient if operating at part-load conditions, but they can become so if working at full load during the entire year.

Other several factors can then affect the return on the investment, among which are the natural gas cost and the discount rate (directly influencing the net present value) and the ambient temperature (influencing the performance and indirectly the net present value). Studies dedicated to the parametric analysis of these factors are already proposed by the authors for what concerns the ORC industrial WHR application (as the reader can find in [19]). Future works are instead under development to focus deeply on investigating these aspects focusing on the s-CO_2 systems only.

7. Conclusions

This paper presents a detailed investigation and comparison of ORC and s-CO_2 potential as bottoming recovery cycles in combined heat and power plant configuration inside industrial facility, comparing several gas turbine models at part-load operation. The findings of this work can be summarized as follows:

- Despite the ORC presenting higher heat recovery efficiency, the s-CO_2 demonstrates better exploitation of the recovered thermal power, showing higher bottoming cycle efficiency, up to the 28%. The ORC efficiency instead does not exceed the 18%. The ORC specific work is considerably affected by the condensing temperature, which determines the condensing pressure and the expander pressure ratio, consequently. This is not valid for the s-CO_2 pressure ratio, which does not depend on the thermal user requested temperature, making the s-CO_2 most suitable for combined heat and power plant applications. The s-CO_2 thermal efficiency is also greater than that of the ORC, with largely positive PES values, up to 22%).
- At part-load operation, an influence of the gas turbine regulation strategy over the bottoming cycles' performance can be observed. In particular, the s-CO_2 system maintains higher part-load performance when working with turbines regulated by means of the VTIT strategy, thus working with almost constant exhaust flow rate. On the contrary, the ORC power plant benefits from working with exhaust temperatures that do not change significantly with respect to the design values.
- In economic terms, the total plant investment cost results in being conspicuous for the s-CO_2 rather than for the ORC. The s-CO_2 requires very higher heat exchangers costs, because of the large size of the heat recovery heat exchanger, but also to the high specific investment cost still associated to this component. The s-CO_2 also requires larger size and more expensive operating machines. On the other hand, the ORC operates with larger turbines due to the lower densities of the fluid during the expansion process, which entail higher expander investment costs. However, this cost item is not counterbalanced by the previous.
- Considering the analyzed scenarios, the high investment costs still associated with the s-CO_2 technology make it already not practical for industrial gas turbine heat recovery applications (no return on the investment), except in the case where a high value carbon tax value is applied. On the contrary, the current lower ORC investment costs make this solution profitable, granting a return on the investment in most of the cases. However, given the considerable economic gain, it is not excluded that once the technology will be established, the s-CO_2 may become very competitive in this sector. Nowadays, a crucial parameter determining the feasibility of the investment is surely the carbon tax value. The influence of the user profile demand is instead less strong, even if it can be decisive when the investment is uncertain and the net present value close to zero.

Nomenclature

Acronyms and Abbreviations

CHP	Combined Heat and Power
GT	Gas Turbine
HX	Heat Exchanger
Norm.	Normalized
ORC	Organic Rankine Cycle
Op.	Operating
s-CO$_2$ PES	Supercritical CO$_2$ Cycle
VIGV	Primary Energy Saving
VSS	Variable Inlet Guide Vanes
VTIT	Variable Shaft Speed
WHR	Variable Turbine Inlet Temperature Waste Heat Recovery

Symbols and Greek letters

A	Heat transfer area (m^2)
C	Cost (EUR)
CF	Cash flow (EUR)
$corr$	Correction factor
E	Energy (Wh/year)
F	Power introduced with fuel (W)
FF	Flow function
h	Enthalpy (J/kg)
I	Total investment (EUR)
LHV	Lower heating value (J/kg)
$\dot{m}$	Mass flow rate (kg/s)
NPV	Net Present Value (EUR)
p	Pressure (bar)
P	Electrical power (W)
PB	Payback period (years)
q	Discount rate (-)
Q	Thermal power (W)
SP	Turbine size parameter (m)
PES	Primary energy saving (-)
T	Temperature (K)
U	Heat transfer coefficient (W/m^2/K)
x_C	Carbon fraction (-)
Δ	Difference
ε	Heat recovery efficiency (-)
η	Efficiency (-)

Subscripts

amb	Ambient
ava	Available
bott	Bottomer
cog	Cogenerative
des	Design
ex	Exhaust gas
exp	Expander
is	Isentropic
mac	Machine
ml	Mean logarithmic
out	Outlet
rec	Recovery
ref	Reference

References

1. IEA. *World Energy Outlook 2019*; IEA: Paris, France, 2019. Available online: https://www.iea.org/reports/world-energy-outlook-2019 (accessed on 17 March 2021).
2. Hedman, B.A. *Waste Energy Recovery Opportunities for Interstate Natural Gas Pipelines*; Interstate Natural Gas Association of America (INGAA): Washington, DC, USA, 2008.
3. Branchini, L.; Bignozzi, M.C.; Ferrari, B.; Mazzanti, B.; Ottaviano, S.; Salvio, M.; Toro, C.; Martini, F.; Canetti, A. Cogeneration Supporting the Energy Transition in the Italian Ceramic Tile Industry. *Sustainability* **2021**, *13*, 4006. [CrossRef]
4. *Thermoflex 29.0*; Thermoflow Inc: Sudbury, MA, USA, 2020.
5. Bianchi, M.; Branchini, L.; de Pascale, A.; Peretto, A. Application of Environmental Performance Assessment of CHP Systems with Local and Global Approaches. *Appl. Energy* **2014**, *130*, 774–782. [CrossRef]
6. Olympios, A.V.; Pantaleo, A.M.; Sapin, P.; Markides, C.N. On the value of combined heat and power (CHP) systems and heat pumps in centralised and distributed heating systems: Lessons from multi-fidelity modelling approaches. *Appl. Energy* **2020**, *274*, 115261. [CrossRef]
7. Li, L.; Mu, H.; Gao, W.; Li, M. Optimization and analysis of CCHP system based on energy loads coupling of residential and office buildings. *Appl. Energy* **2014**, *136*, 206–216. [CrossRef]
8. Redko, A.; Redko, O.; DiPippo, R. (Eds.) 9-Industrial waste heat resources. In *Low-Temperature Energy Systems with Applications of Renewable Energy*; Academic Press: Cambridge, MA, USA, 2020; pp. 329–362. ISBN 978-0-12-816249-1.
9. Macchi, E.; Astolfi, M. (Eds.) *Organic Rankine Cycle (ORC) Power Systems: Technologies and Applications*; Woodhead Publishing Series in Energy; Woodhead Publishing is an Imprint of Elsevier: Sawston, UK; Cambridge, UK, 2017; ISBN 978-0-08-100510-1.
10. White, M.T.; Bianchi, G.; Chai, L.; Tassou, S.A.; Sayma, A.I. Review of Supercritical CO_2 Technologies and Systems for Power Generation. *Appl. Therm. Eng.* **2021**, *185*, 116447. [CrossRef]
11. Tartière, T.; Astolfi, M. A World Overview of the Organic Rankine Cycle Market. *Energy Procedia* **2017**, *129*, 2–9. [CrossRef]
12. Analysis of the Organic Rankine Cycle Market. Available online: https://orc-world-map.org/analysis.html (accessed on 23 March 2021).
13. Campana, F.; Bianchi, M.; Branchini, L.; De Pascale, A.; Peretto, A.; Baresi, M.; Fermi, A.; Rossetti, N.; Vescovo, R. ORC Waste Heat Recovery in European Energy Intensive Industries: Energy and GHG Savings. *Energy Convers. Manag.* **2013**, *76*, 244–252. [CrossRef]
14. Semmari, H.; Filali, A.; Aberkane, S.; Feidt, R.; Feidt, M. Flare Gas Waste Heat Recovery: Assessment of Organic Rankine Cycle for Electricity Production and Possible Coupling with Absorption Chiller. *Energies* **2020**, *13*, 2265. [CrossRef]
15. Song, J.; Li, Y.; Gu, C.; Zhang, L. Thermodynamic analysis and performance optimization of an ORC (Organic Rankine Cycle) system for multi-strand waste heat sources in petroleum refining industry. *Energy.* **2014**, *71*, 673–680. [CrossRef]
16. Matuszewska, D.; Olczak, P. Evaluation of Using Gas Turbine to Increase Efficiency of the Organic Rankine Cycle (ORC). *Energies* **2020**, *13*, 1499. [CrossRef]
17. CEO Recycled Energy Market Overview—Updated 2017.Pdf. Available online: https://drive.google.com/file/d/1lw-EQkpIhs6ZemFRtARh6Gv5hwVe5Amt/view?usp=drive_open&usp=embed_facebook (accessed on 8 June 2021).
18. EPS100 | Echogen Power Systems. Available online: https://www.echogen.com/our-solution/product-series/eps100/ (accessed on 11 January 2021).
19. Bianchi, M.; Branchini, L.; De Pascale, A.; Melino, F.; Peretto, A.; Archetti, D.; Campana, F.; Ferrari, T.; Rossetti, N. Feasibility of ORC Application in Natural Gas Compressor Stations. *Energy* **2019**, *173*, 1–15. [CrossRef]
20. Zhou, A.; Li, X.; Ren, X.; Gu, C. Improvement Design and Analysis of a Supercritical CO2/Transcritical CO2 Combined Cycle for Offshore Gas Turbine Waste Heat Recovery. *Energy* **2020**, *210*, 118562. [CrossRef]
21. Astolfi, M.; Alfani, D.; Lasala, S.; Macchi, E. Comparison between ORC and CO2 Power Systems for the Exploitation of Low-Medium Temperature Heat Sources. *Energy* **2018**, *161*, 1250–1261. [CrossRef]

22. Yoon, S.Y.; Kim, M.J.; Kim, I.S.; Kim, T.S. Comparison of Micro Gas Turbine Heat Recovery Systems Using ORC and Trans-Critical CO_2 Cycle Focusing on off-Design Performance. *Energy Procedia* **2017**, *129*, 987–994. [CrossRef]

23. Ancona, M.A.; Bianchi, M.; Branchini, L.; De Pascale, A.; Melino, F.; Peretto, A.; Torricelli, N. A Comparison Between ORC and Supercritical CO_2 Bottoming Cycles for Energy Recovery from Industrial Gas Turbines Exhaust Gas. In Proceedings of the ASME Turbo Expo 2021. virtual event. (Accepted manuscript—in press).

24. Bhargava, R.K.; Bianchi, M.; Branchini, L.; De Pascale, A.; Orlandini, V. Organic Rankine Cycle System for Effective Energy Recovery in Offshore Applications: A Parametric Investigation with Different Power Rating Gas Turbines. In Proceedings of the ASME Turbo Expo 2015, Montreal, QC, Canada, 15–19 June 2015. [CrossRef]

25. Crespi, F.; Gavagnin, G.; Sánchez, D.; Martínez, G.S. Analysis of the Thermodynamic Potential of Supercritical Carbon Dioxide Cycles: A Systematic Approach. *J. Eng. Gas Turbines Power* **2018**, *140*, 051701. [CrossRef]

26. Ahn, Y.; Lee, J.; Kim, S.G.; Lee, J.I.; Cha, J.E.; Lee, S.-W. Design Consideration of Supercritical CO_2 Power Cycle Integral Experiment Loop. *Energy* **2015**, *86*, 115–127. [CrossRef]

27. Lemmon, E.W.; Bell, I.H.; Huber, M.L.; McLinden, M.O. *McLinden REFPROP 10.0 Standard Reference Database 23*; National Institute of Standards and Technology: Gaithersburg, MD, USA, 2021.

28. Directive 2004/08/EC of the European Parliament and of the Council, Official Journal of the European Union 21.2.2004; pp. 50–60. Available online: https://eur-lex.europa.eu/LexUriServ/LexUriServ.do?uri=OJ:L:2004:052:0050:0060:EN:PDF (accessed on 4 November 2020).

29. Green, D.W.; Southard, M.Z. *Perry's Chemical Engineers' Handbook*, 9th ed.; McGraw-Hill Education: Manhattan, NY, USA, 2019; ISBN 978-0-07-183408-7.

30. Weiland, N.T.; Lance, B.W.; Pidaparti, S.R. SCO2 Power Cycle Component Cost Correlations from DOE Data Spanning Multiple Scales and Applications. In Proceedings of the ASME Turbo Expo 2019, Phoenix, AZ, USA, 17–21 June 2019. [CrossRef]

31. Astolfi, M.; Romano, M.C.; Bombarda, P.; Macchi, E. Binary ORC (Organic Rankine Cycles) Power Plants for the Exploitation of Medium–Low Temperature Geothermal Sources—Part B: Techno-Economic Optimization. *Energy* **2014**, *66*, 435–446. [CrossRef]

32. Marchionni, M.; Bianchi, G.; Tassou, S.A. Review of Supercritical Carbon Dioxide (SCO2) Technologies for High-Grade Waste Heat to Power Conversion. *SN Appl. Sci.* **2020**, *2*, 611. [CrossRef]

33. NIST Repository-Thermodynamic Properties of Natural Gas and Related Gases. Available online: https://pages.nist.gov/AGA8/ (accessed on 6 May 2021).

34. Statistics | Eurostat. Available online: https://ec.europa.eu/eurostat/databrowser/view/nrg_pc_203/default/table?lang=en (accessed on 19 April 2021).

35. European Countries with a Carbon Tax | Tax Foundation. Available online: https://taxfoundation.org/carbon-taxes-in-europe-2020/ (accessed on 19 April 2021).

36. Kurz, R.; Ohanian, S.; Lubomirsky, M. On Compressor Station Layout. In Proceedings of the ASME Turbo Expo 2003, Atlanta, GA, USA, 16–19 June 2003; pp. 1–10. [CrossRef]